CHAPTER 6

MECHANISM OF MASS TRANSFER

Mass Transfer Model

Boey (1989) and Chaudhuri (1990) summarized the mechanism of mass transfer in liquid membrane as follows.

Mechanism of mass transfer in liquid membrane systems have been proposed in the literature to explain and predict the rate of solute transfer and the effect of operating parameters. The literature available on supported liquid membrane is vast. The mass transfer model for the emulsion liquid membrane, in the main, is extended from the model of supported liquid membranes:

1. The phases on either side of the membrane are well mixed, therefore mass transfer resistance is negligible.

2. The membrane phase is stagnant.

3. The system is at steady state.

4. The diffusion coefficients in the membrane phase are constant.

5. Chemical equilibrium exists at both interface.

In most cases an "effective" diffusivity is used to account for the tortuous path of the diffusing species through the inert support.

Various model have been proposed for emulsion liquid membranes. Many of these models are developed for Unfacilitated Transport, but are also equally

applicable for Facilitated Transport by assuming that the diffusion of the carrier complex across the membrane phase is rate limiting.

The five models that have been developed so far will be briefly described as follows.

1. Uniform Flat Sheet Model.

In this model, all the internal phase droplets containing the stripping reagents are coalesced into one large droplet. The membrane phase thickness is assumed to be so small in comparison with the globule diameter that the mass transfer area in the direction of solute transport can be considered constant , i.e. planar geometry can be assumed. It is further assumed that the phases on either side of the membrane are well mixed, while the membrane phase itself is stagnant. Thus the model is similar to that of the supported liquid membrane.

2. Hollow Sphere Model.

This model is similar to the Uniform Flat Sheet Model but allows for the spherical geometry of the system. Thus the internal droplets are also assumed to be coalesced into a single well mixed droplet, but here, a spherical membrane of finite thickness surrounds this droplet.

3. Hollow Sphere-Advancing Front Model.

This model follows the lines of the Hollow Sphere Model, except that, here, no mixing is assumed within the internal droplet. As a consequence, the diffusing species is removed first by the internal reagent adjacent to the membrane phase, and then has to penetrate further into the droplet as the reagent is consumed. Thus,

a concentric reaction advances towards the center of the droplets as the stripping reaction progresses.

4. Immobilized Globule-Advancing Front Model.

This model is by far the most realistic in terms of geometry and configuration of the emulsion globule. The internal droplets are allowed to retain their identity. The model further assumes that:

a) There is no circulation of the droplets, i.e. they are immobilized or fixed in space.

b) There is local chemical equilibrium between the membrane phase and the internal phase.

This model is commonly known as "Shrinking Core Model". The solute diffuses through the membrane phase where upon it is removed by an irreversible chemical reaction in the internal droplets. A reaction front develops that advances into the center of the globules as the reagent within the outermost droplets is consumed.

5. Immobilized Hollow Spherical Globule-Advancing Front Model.

This is similar to the above model in that the internal droplets are also allowed to retain their shape and identity. A further assumption made, is that a thin distinct layer of membrane phase fluid surrounds the globule. A mass transfer resistance is assigned to this layer.

Literature on Proposed Model for Emulsion Liquid Membrane.

Over the past few years, while many papers have experimentally demonstrated the possibility of applying emulsion liquid membrane to separate various species, only a few papers have dealt with the mathematical modeling of such process.

Early attempts at modeling of real systems adopted the flat sheet model for its simplicity. Cahn and Li (1974) modeled unfacilitated transport of phenol in emulsion liquid membranes in which the extraction rate was assumed to be proportional to the solute concentration difference between the internal and the external phase.

Matulevicius and Li (1975) proposed a hollow sphere model in which the mass transfer resistance was assumed to be limited to the peripheral shell of the emulsion globules and kept constant during the extraction process to describe phenol extraction by emulsion liquid membrane.

Another improved approach, but more mathematically complex model, is to assume that the internal encapsulated droplets are immobilized and homogeneously distributed in the emulsion globule. This approach accounts for mass transfer contributions accompanying solute diffusing and reacting in an emulsion globule. Ho et.al. (1982), used this approach to analyze the phenol removal from waste water system. They assumed that solute removed from the bulk phase diffused through the globule to a reaction front, where it was removed instantaneously and irreversibly by reaction with an internal reagent. The reaction front advances towards the center as the reagent is consumed.

Teramoto et.al. (1983) have developed models which incorporated the more realistic assumption of reaction equilibrium. In the reversible reaction model locating the reaction front is unnecessary.

There has been more success with this model in explaining experimental results, this basic model has been extended to account for poly dispersity of the internal phase droplets (Lobarch and Hatton, 1988) and reaction reversibility in Unfacilitated Transport (Baird et.al.,1987).

Terramoto et.al. (1991) proposed a permeation model for the extraction of tryptophan, phenylalanine and β-phenethylamine on the basis of immobilized hollow spherical globule-advancing front model, in which diffusional processes in the external aqueous phase and in the w/o emulsion globules, as well as extraction equilibrium, are considered. They concluded that the experimental results were satisfactorily simulated by the proposed model.

Mechanism of Mass Transfer of Amino Acid.

The objective of this study concerning the mechanism of mass transfer of amino acid is to obtain the influence of external pH on the permeation rate by simulation.

Eventhough the advancing front model seemed to be regarded as the most realistic model used to represent emulsion liquid membrane system. Many assumptions and unknown parameters are required in the model. Many experiments have to be performed in order to get the values of parameters that can be applied in any certain condition. The mechanism of mass transfer of amino acid in emulsion

liquid membrane seems to be very complicated especially on the surface area of mass transfer. It involves many small droplets of globules which sizes vary with stirring conditions and it also very difficult to measure the diameter in order to get accurate values. Furthermore, during extraction the swelling and breakage of the emulsion will occur. These phenomena make the system more complicated. At present, no model can really describe the mechanism of mass transfer in emulsion liquid membrane served many assumptions. Therefore, the simplest model will be proposed in this study.

The simplest model is the uniform flat sheet model, as described above. From the study of equilibrium extraction of L-lysine in chapter 4, the following equations can be obtained:

$$A^{2+} + m\overline{(HR)} \longleftrightarrow \overline{AR_m} + H^{+} \qquad \text{..... (6.1)}$$

The schematic diagram of the permeation mechanism of amino acid through a liquid membrane containing D2EHPA as a cation carrier is illustrated in figure 6-3. Amino acid ion in the feed solution diffuse toward the interface (x=0), where complex formation between 12 moles of amino acid ion and 1 mole of dimeric D2EHPA occurs. This complex $A_{12}R$ then diffuses through the membrane toward the interface x=1, where amino acid ion is stripped back to the stripping solution. This step regenerates the D2EHPA carrier which then diffuses back to the interface x=0, after which the entire process is repeated. Such a process is called "counter-transport". It is able to transport amino acid ion from a low concentration solution to a high concentration solution.

The concentration profile across the permeation cell is schematically shown in figure 6-4. It is assumed that linear concentration gradients exist throughout the system. The resistance of hydrogen ion diffusion in both aqueous solutions and of amino acid ion in the stripping solution are also assumed to be negligible.

In quasi-study state, the permeation rates of amino acid are involved the following equation:

1. Permeation rate of amino acid in the feed phase

$$J_{A,f} = \frac{(D_{A,f})}{\delta} ([A^+]_f - [A^+]_o) \quad \cdots\cdots\cdots\cdots \quad (6.2)$$

$$J_{A,f} = (k_{A,f}) ([A^+]_f - [A^+]_o) \quad \cdots\cdots\cdots\cdots \quad (6.3)$$

2. Interfacial reaction rate at the interface between feed phase and membrane phase

$$R_1 = k_1 [A^+]_o [(\overline{HR})]^{0.12}_o - k_{-1} [\overline{A^+}]_o [H^+]_o \quad \cdots\cdots\cdots\cdots \quad (6.4)$$

3. Permeation rate of amino acid complex in the membrane phase and stripping phase.

$$J_C = \frac{(D_C)}{\tau l} ([\overline{A^+}]_o - [\overline{A^+}]_l) \quad \cdots\cdots\cdots\cdots \quad (6.5)$$

4. Interfacial reaction rate at the interface between membrane phase and stripping phase.

$$R_{-1} = k_1 [\overline{A^+}]_l [H^+]_l - k_1 [A^+]_l [(\overline{HR})]_l^{0.12} \quad \cdots\cdots\cdots\cdots \quad (6.6)$$

5. Permeation rate of amino acid in the stripping phase.

$$J_{A,s} = \frac{(D_{A,s})}{\delta} ([A^+]_l - [A^+]_s) \quad \text{----------} \quad (6.7)$$

$$J_{A,s} = (k_{A,s}) ([A^+]_l - [A^+]_s) \quad \text{----------} \quad (6.8)$$

where J_A : permeation rate of amino acid in the aqueous phase.

D_A : diffusivity of amino acid.

D_C : diffusivity of amino acid/D2EHPA complex.

$[A^+]$: cation of amino acid

$\overline{[A^+]}$: concentration of amino acid/D2EHPA complex or $AR(HR)_3$ in the membrane phase.

$\overline{(HR)}$: monomeric form of D2EHPA in the membrane phase.

τ : membrane constant.

l : thickness of the membrane.

δ : Thickness of the aqueous film.

k_1, k_2 : interfacial reaction rate constant.

Subscripts f, o, l, and s refer to positions shown in figure 6-4.

When the quasi-steady state is reached,

$$J = J_{A,f} = R_l = J_C = R_{-l} = J_{A,s}$$

From equation (6.2) to (6.8), the following equation (6.8) permeation rate of amino acid can be derived based on the assumption that all species have an equal

diffusivity in the membrane and D2EHPA carrier and the amino acid/D2EHPA complex are soluble only in the liquid membrane.

$$J = \frac{\frac{[\overline{(HR)}]^{0.12}{}_0[A^+]_f}{[H^+]_0} - \frac{[\overline{(HR)}]^{0.12}{}_l[A^+]_s}{[H^+]_l}}{\frac{[\overline{(HR)}]^{0.12}{}_0}{k_{A\,f}[H^+]_0} + \frac{1}{k_l}\left\{\frac{1}{[H^+]_0} + \frac{1}{[H^+]_l}\right\} + \frac{[\overline{(HR)}]^{0.12}{}_l}{k_{A\,s}[H^+]_l} + \frac{k_{-l}(tl)}{kD_C}} \quad \cdots\cdots\cdots (6.9)$$

If the membrane diffusion control is assumed in this case the permeation rate of amino acid will be as follow:

$$J = \frac{k_l}{k_{-l}} \frac{D_C}{tl} \frac{[(HR)]^{0.12}{}_0[A^+]_f}{[H^+]_0} - \frac{[(HR)]^{0.12}{}_l[A^+]_s}{[H^+]_l} \quad \cdots\cdots\cdots (6\text{-}10)$$

Since; $K_{ex} = \frac{k_l}{k_{-l}}$

$$J = K_{ex} \frac{D_C}{tl} \frac{[(HR)]^{0.12}{}_0[A^+]_f}{[H^+]_0} - \frac{[(HR)]^{0.12}{}_l[A^+]_s}{[H^+]_l} \quad \cdots\cdots\cdots (6\text{-}11)$$

At the very initial state of extraction, $[A^+]_s$ can be assumed to be zero.

Therefore, the equation will be:

$$J = \frac{D_C}{tl} \frac{K_{ex}[(HR)]^{0.12}{}_0[A^+]_f}{[H^+]_0} \quad \cdots\cdots\cdots (6\text{-}12)$$

Equation (6.12) is the very simple model equation to predict the influence of external pH on the permeation rate at the initial state of extraction.

From this simple model, it was found that the permeation rate of amino acid is inversely proportional to the initial pH value of feed phase. The initial extraction rate of amino acid at lower pH will be less than the initial extraction rate of amino

acid at higher pH. This prediction is true in the real extraction. Therefore, the trend from the influence of pH in the feed solution on the permeation rate can be obtained from this simple permeation model.

The results of calculations of on initial permeation rate of 0.01 M L-lysine at pH 2, 3, 4, 5, and 6 from the model equation and experimental data are summarized in Table 6-1. The initial permeation rates (J/D_c ,mol/m^4) at pH 2, 3, 4, 5, and 6 which were calculated from equation (6.12) are shown in Figure 6-1. As shown in Figure 6-2, Jxa is plotted against pH. In this case "a" which is the mass transfer area of liquid membrane was assumed to be constant. Figure 6-2 shows results from the experimental data which shows a similar trend as in Figure 6-1. However, the results from the experimental data shows some variation from the model equation, this both in the internal and external aqueous phase. The other reason for this variation may be from the experimental data that are used for initial rate conclude that the initial permeation rate at pH 5 is the best. The prediction of initial permeation rate tend from the model equation shows the similar result as from experimental data.

Sample of Calculations

In carrier variation, the results of calculation on initial permeation rate of 0.01 M L-lysine at various carrier concentrations from model equation and experimental data are summarized in Table 6-2. The initial permeation rates (J/D_c ,mol/m^4) at various concentrations of carrier which were calculated from equation (6.12) are shown in Figure 6-3. As shown in Figure 6-4, Jxa is plotted against carrier concentration. Figure 6-4 shows results from the experimental data which shows

similar trend as in Figure 6-3. However, the prediction of initial permeation rate tend from the model equation shows the similar result as from experimental data.

Example of Calculation

According to equation (6.12), the permeation rate at the initial state can be calculated as follows:

1.Calculation of $[A^{\pm}]$ in the Feed Phase.

A_T : $A^{2+} + A^{+}$ ..... (a)

where A_T : Total amount of amino acid = 0.01 M

A^{2+} : two cation of amino acid

A^{+} : cation of amino acid

$$K_1 = \frac{[A^+][H^+]}{[A^{2+}]} \quad \text{..... (b)}$$

where K_1 : Dissociation constant of amino acid, mol/dm^3

K_1 for l-lysine = $10^{-2.18}$ mol/dm^3

At pH 2.0,

$$10^{-2.18} = \frac{[A^+][10^{-2}]}{[A^{2+}]}$$

$$[A^+] = 0.66[A^{2+}] \quad \text{..... (c)}$$

From (a) ; 0.01 M = $[A^{2+}]$ + $[A^+]$ ..... (d)

From (c) and (d) ; $[A^{2+}] = 6.02 \times 10^{-3}$ mol/dm^3

Therefore, $[A^{2+}]$ in the feed phase at pH 2.0 = 6.02 mol/m^3

2. Calculation of Membrane Thickness

In this experiment, 50 ml of internal phase and 50 ml of membrane phase was emulsified to make the emulsion.

Based on the assumption that the initial phase is coalesced into a single droplet with volume of 50 ml and the outer spherical droplet will be 100 ml in volume, the thickness of the membrane(l) can be calculated as follow:

a) Diameter of Inner Sphere (D_i)

Volume of inner sphere = $0.050\ dm^3$

$$\frac{1}{6}\pi D_i^3 = 0.050 \times 10^{-3}\ m^3$$

$$D_i = \sqrt[3]{0.050\times10^{-3} \times \frac{6}{\pi}} = 0.0457\ m$$

b) Diameter of Outer Sphere (D_o).

Volume of outer sphere = $0.10\ dm^3$

$$\frac{1}{6}\pi D_o^3 = 0.10 \times 10^{-3}\ m^3$$

$$D_o = \sqrt[3]{0.10\times10^{-3} \times \frac{6}{\pi}}$$

$$D_o = 0.0576\ m$$

$$\text{Membrane thickness (l)} = \frac{D_o - D_i}{2} = \frac{0.0576 - 0.0457}{2}$$

$$= 5.9 \times 10^{-3}\ m.$$

3) Calculation of Permeation rate from the Model Equation.

$$J = \frac{D_C}{tl} \frac{K_{ex}[(HR)]^{0.12}{}_0[A^{2+}]_f}{[H^+]_0} \qquad \text{(6-12)}$$

K_{ex} = 0.2047×10^{-3} m^3/mol (from this study)

(HR) = 0.3100 mol/dm^3 = 310 mol/m^3

$[A^{2+}]_f$ at pH 2.0 = 6.02 mol/m^3

$[H^+]_0$ = $10^{-2} \times 10^3$ mol/m^3

l = 5.9×10^{-3} m

D_C (m^2/s)

τ : assumed to be one.

$$J = \frac{D_C}{(1.0)(5.9\times10^{-3})} \frac{(0.2047\times10^{-3})(310)^{0.12}\,(6.02)}{(10^{-2}\times10^3)} \quad mol/m^2.s$$

J/Dc = $(0.0146)D_c$ mol/s^2

Table 6-1 Calculated and Experimental Value of Initial Permeation Rate of 0.01 M L-lysine at various pH.

pH	Experimental Result J x a (mol/s)	Model Equation J / D_c (mol/m^4)
2	0.0100	0.0416
3	0.0478	0.0908
4	0.0548	0.1030
5	0.0906	0.1044
6	0.0724	0.1045

Table 6-2 Calculated and Experimental Value of Initial Permeation Rate of 0.01 M L-lysine at various carrier concentration.

Carrier concentration (%v/v)	Experimental Result J x a (mol/s)	Model Equation J / D_c (mol/m^4)
3	0.0327	0.0157
5	0.0653	0.0167
7	0.0805	0.0174
10	0.0934	0.0182
15	0.1376	0.0191

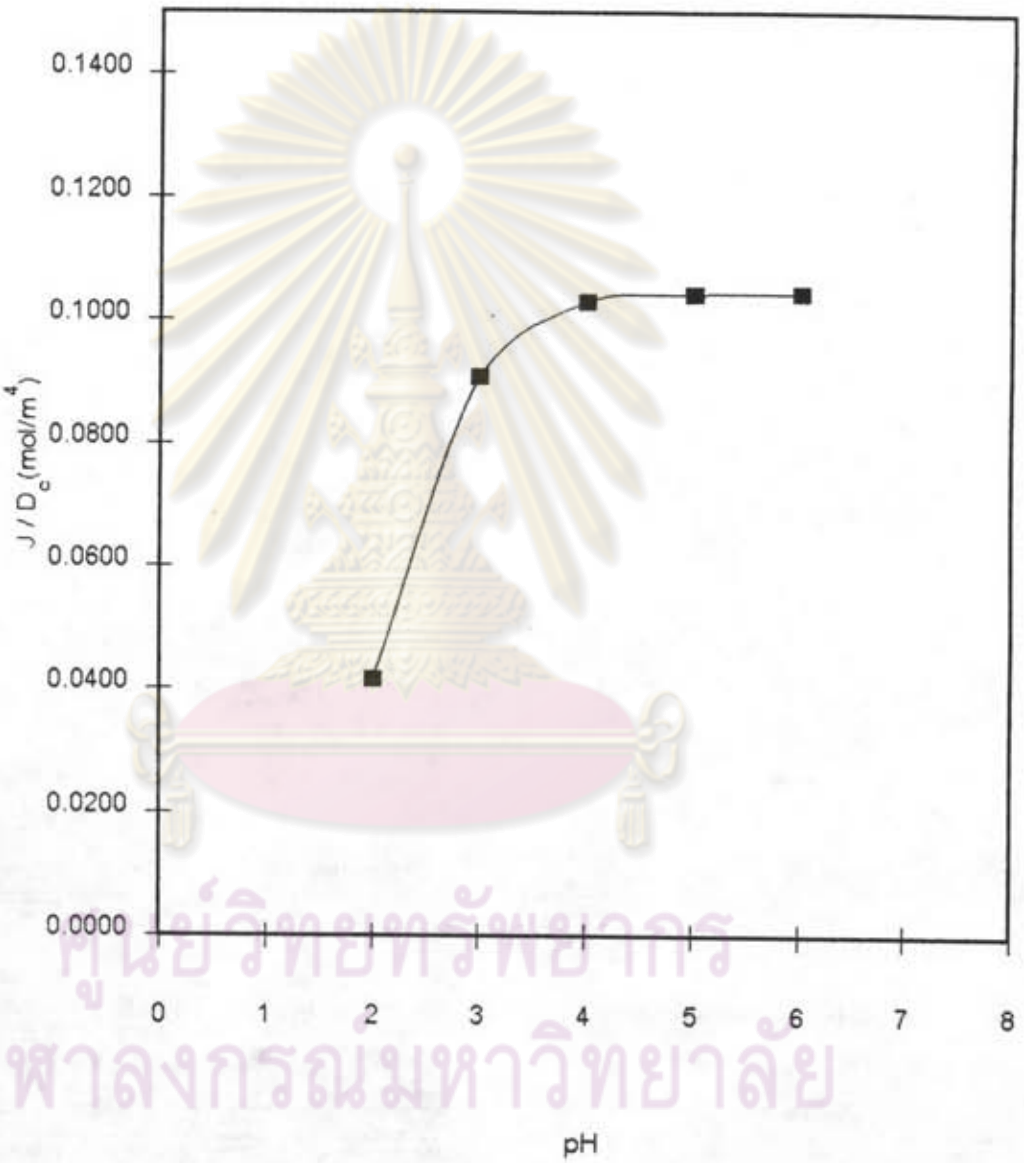

Figure 6-1 J / D_c vs. pH (Model Equation)

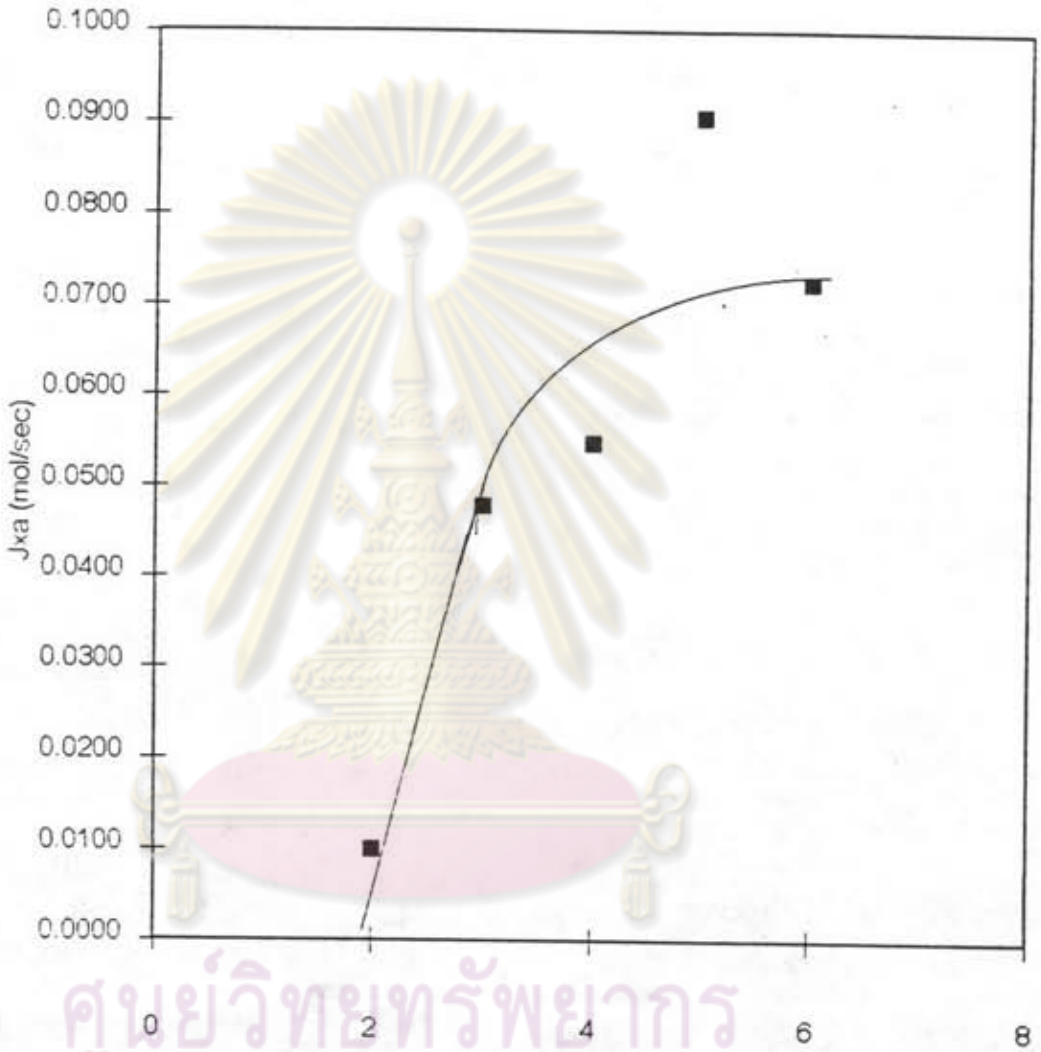

Figure 6-2 Jxa vs. pH (Experimental Result)

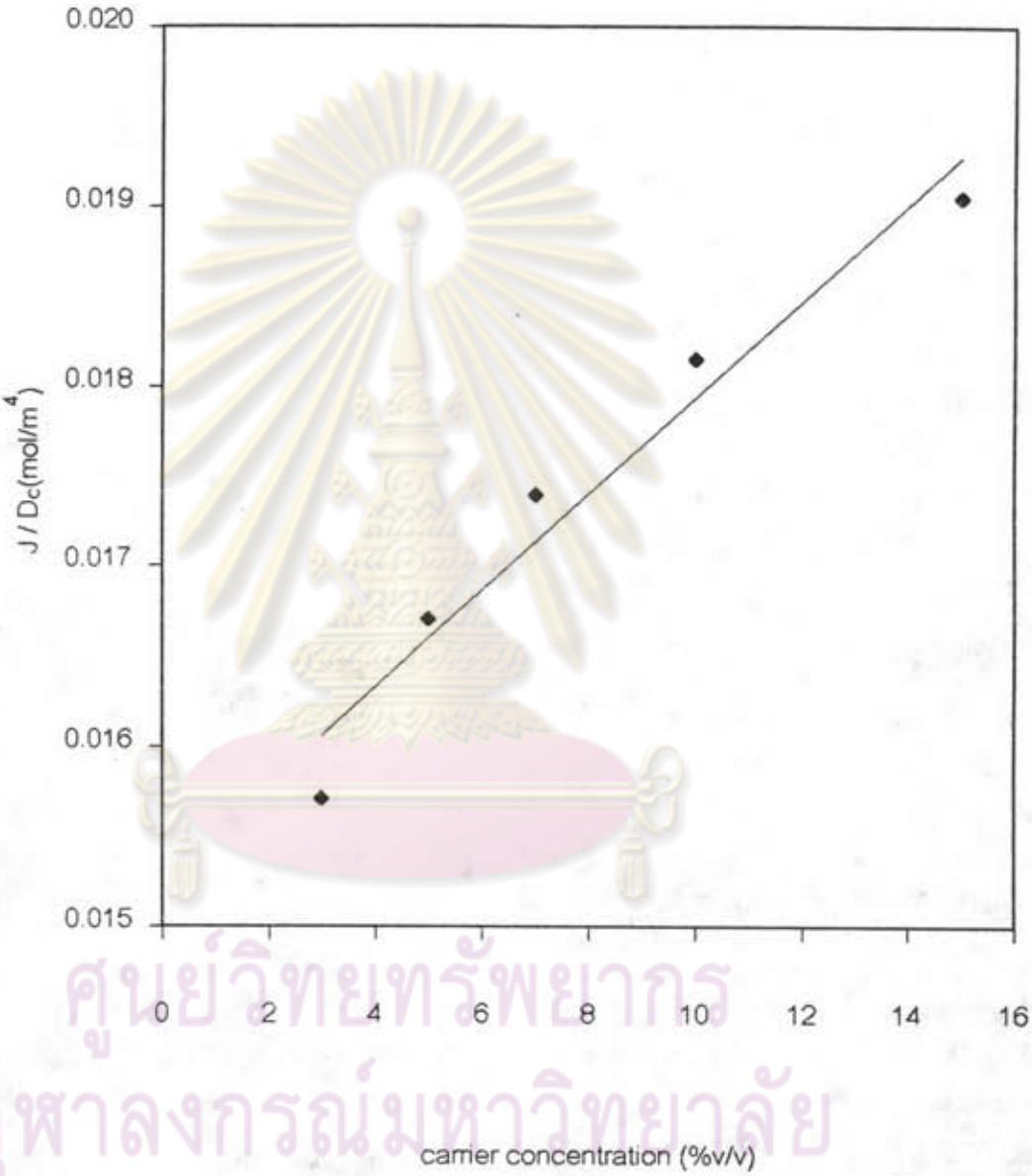

Figure 6-3 J x D_c vs. Carrier Concentration.

(Model equation)

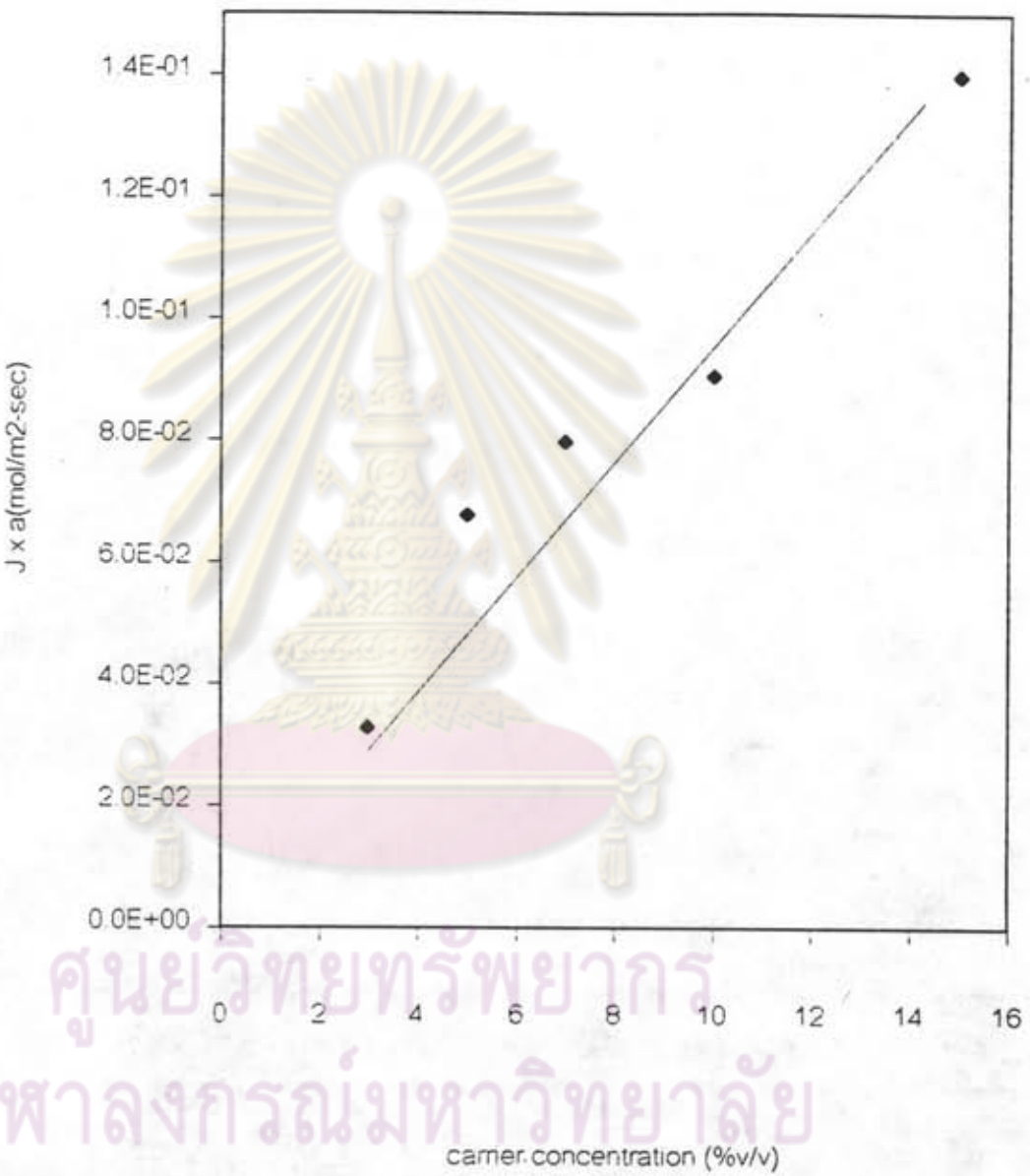

Figure 6-4 J vs Carrier Concentration.

(Experimental result)

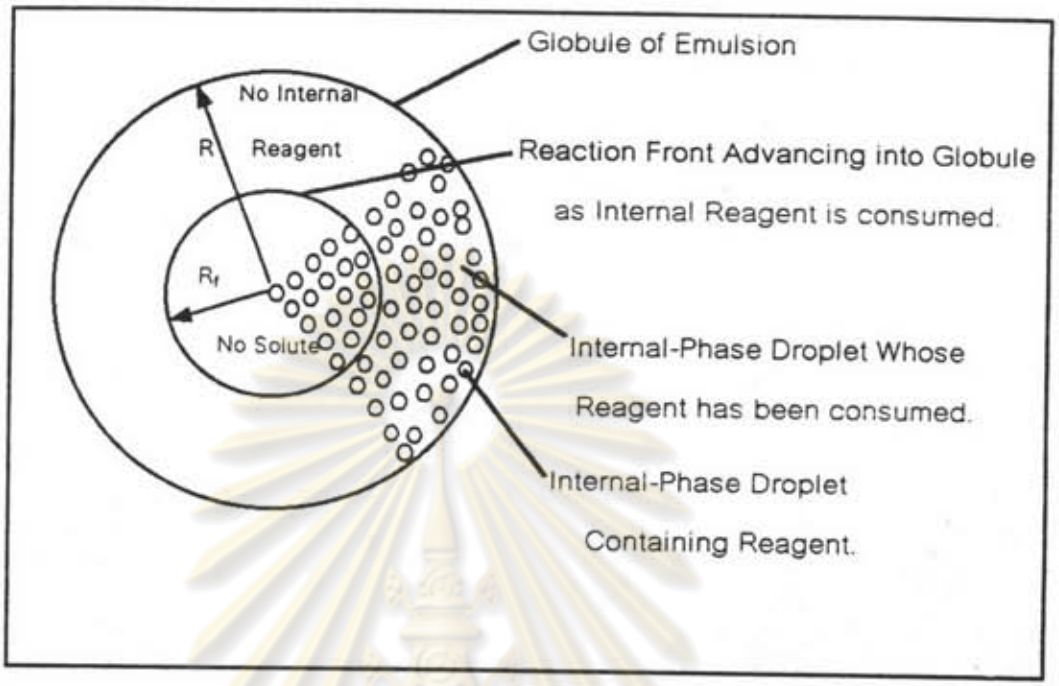

Figure 6-5 Schematic Diagram of Immobilized Globule-Advancing Front Model.

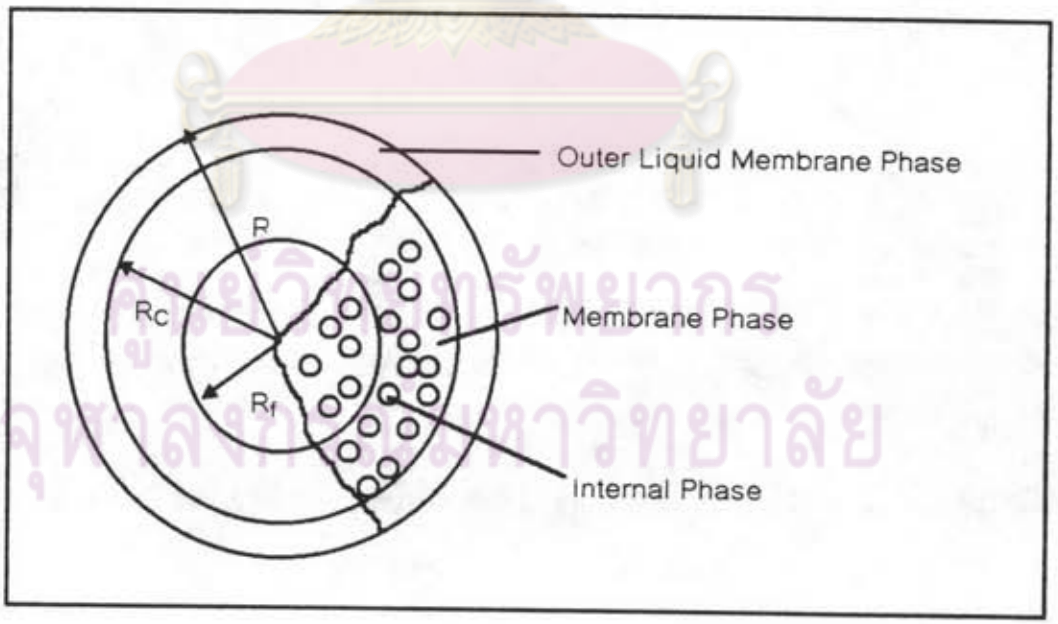

Figure 6-6 Schematic Diagram of Immobilized Hollow Spherical Globule-Advancing Front Model.

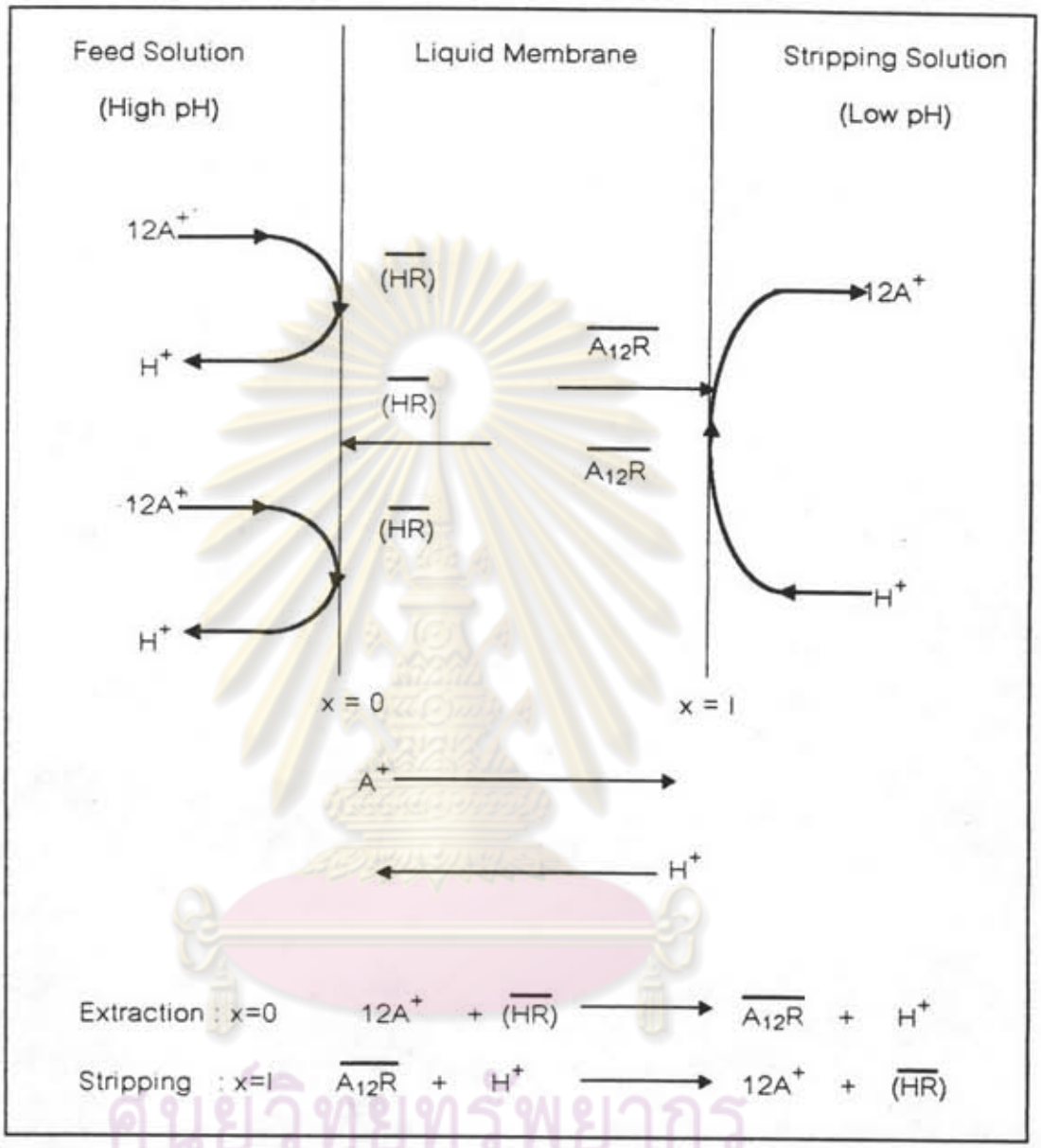

Figure 6-7 Uniform Flat Sheet Model for Amino Acid Permeation.

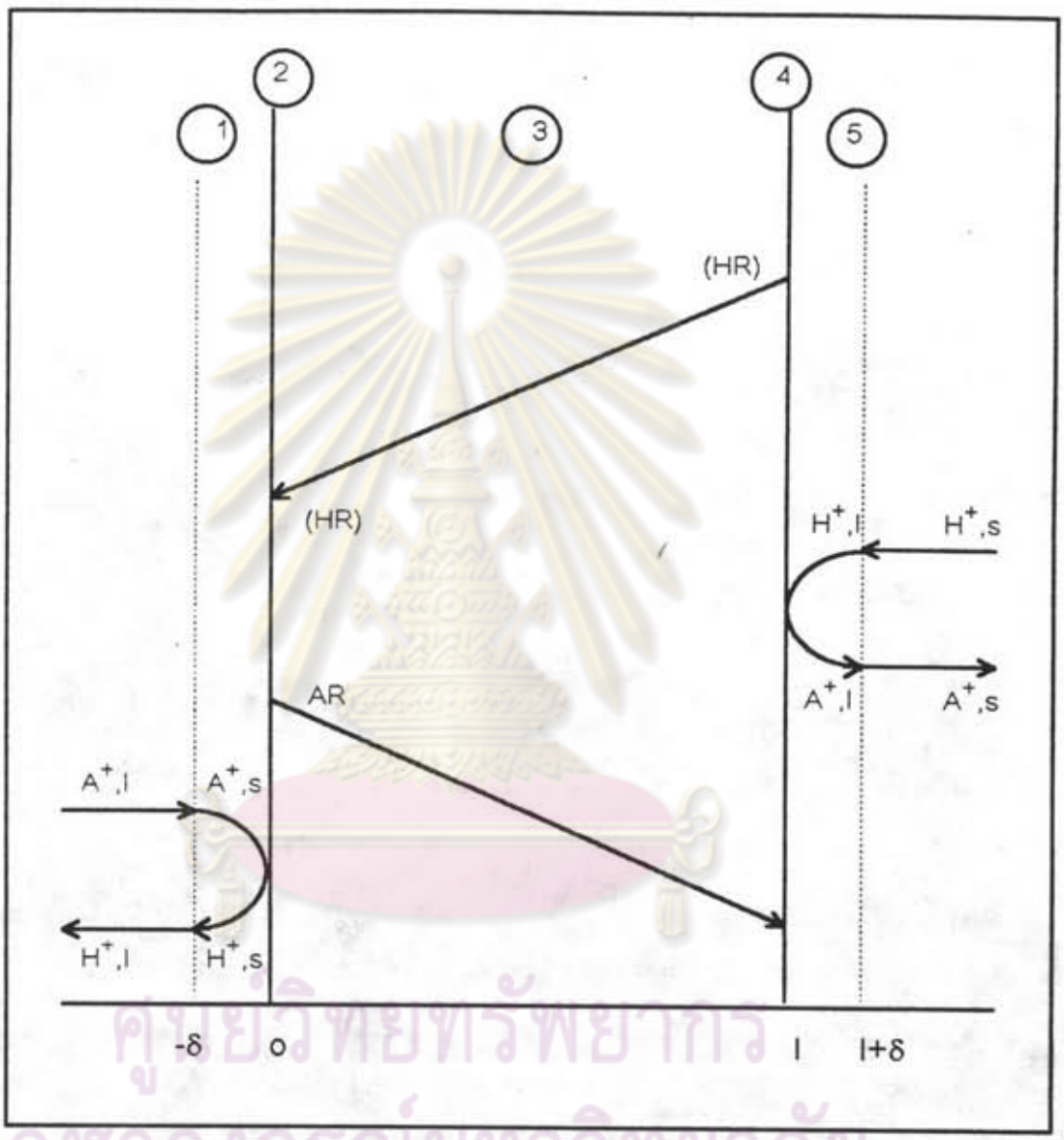

Figure 6-8 Schematic Concentration Profile of Amino Acid Permeation.